Soft Matter

Accepted Manuscript

ROYAL SOCIETY
OF **CHEMISTRY**

www.rsc.org/softmatter

Equation of state and adsorption dynamics of soft microgel particles at an air-water interface

Omkar S. Deshmukh,[a] Armando Maestro,[a‡] Michel H.G. Duits,[a] Dirk van den Ende,[a] Martien Cohen Stuart,[a] and Frieder Mugele,[*a]

Received Xth XXXXXXXXXX 20XX, Accepted Xth XXXXXXXXX 20XX
First published on the web Xth XXXXXXXXXX 200X
DOI: 10.1039/b000000x

Understanding the adsorption dynamics of soft microgel particles is a key step in designing such particles for potential applications as stimuli-responsive Pickering stabilizers for foams or emulsions. In this study we experimentally determine an equation of state (EOS) for Poly (N-isopropylacrylamide) (PNIPAM) microgel particles adsorbed onto an air-water interface using a Langmuir film balance. We detect a finite surface pressure at very low surface concentration of particles, for which standard theories based on hard disk models predict negligible pressures, implying that the particles must deform strongly upon adsorption to the interface. Furthermore, we study the evolution of the surface pressure due to the adsorption of PNIPAM particles as a function of time using pendant drop tensiometry. The equation of state determined in the equilibrium measurements allows us to extract the adsorbed amount as a function of time. We find a mixed-kinetic adsorption that is initially controlled by the diffusion of particles towards the interface. At later stages, a slow exponential relaxation indicates the presence of a coverage-dependent adsorption barrier related to crowding of particles at the interface.

1 Introduction

Microgel particles (swollen colloidal particles consisting of cross-linked soluble polymers) show great promise as Pickering stabilizers of emulsions and foams[1–3]. This has two reasons. First, the fact that they are particles makes them adsorb very strongly to the interface with adsorption energies in order of hundreds of k_BT or more[4]. Second, their swollen polymeric character facilitates attachment from solution to fluid interfaces in comparison to solid particles[4,5]. Understanding how these particles stabilize the interface, what shape they take and what surface pressures they generate are the important questions that need to be addressed in the context of knowledge based design of particles for these specific applications. Although various studies of adsorbed microgel layers have appeared[6–11], none of them has precisely established the equation of state for these adsorbed soft microgel particles. There also exists a dearth of experiments regarding the adsorption dynamics of these particles onto fluid interfaces. Yet, the processes controlling adsorption are at present not well understood. For example, it has been found that the adsorption of hard colloidal particles is strongly affected by the electrostatic interactions between the particles and the air-water interface[12]. Negative particles are repelled and adsorb slowly or not at all (depending on the ionic strength and dynamic conditions) whereas positive particles adsorb readily, possibly following a diffusion based rate law. It is not yet known whether the adsorption of soft particles is governed by similar processes. Even the equilibrium surface pressure as a function of the amount of adsorbed soft particles, *i.e.* the equation of state (EOS) is poorly known, let alone the physical mechanism giving rise to surface pressure. It is well-known that a 2D ideal gas model of adsorbed colloidal particles will not lead to a measurable pressure due to the large size of the particles[8]. Hence a simple 2D hard disk model will predict measurable pressures only for adsorbed layers extremely close to the hexagonal close packing limit. Groot and Stoyanov[13] carried out dissipative particle dynamics (DPD) simulations of soft particles at fluid interfaces and proposed to rescale the density by introducing an effective length scale, which is two orders of magnitude smaller than the particle size. This leads to more realistic values of the surface pressure, yet the physical meaning of this effective length is not very clear.

Finally it is important to realize that such soft microgel particles deform strongly upon adsorption to both solid - liquid[14] and liquid - liquid[3,7,15,16] interfaces resulting in ‘sombrero’ or ‘fried egg-like’ morphologies. In the case of fluid - fluid interfaces, this deformation is usually attributed to the tendency of the polymer strands to maximize their contact with the interface counteracted by the particle elasticity. The extent of deformation is then controlled by $\Delta\gamma/\epsilon$, where $\Delta\gamma$ is the net interfacial tension acting on the particle and ϵ is the Young’s

---

[a] *Physics of Complex Fluids, Dept. Science and Technology, University of Twente, PO Box 217, 7500AE, Enschede, The Netherlands.*
[*] *Corresponding author - Fax: +31 53 4893094; Tel: +31 53 4891096; E-mail: f.mugele@utwente.nl*
‡*Current Address: Cavendish Laboratory, University of Cambridge, JJ Thompson Avenue, CB3 0EH Cambridge, UK*

modulus of the particles. For swollen particles at the air-water interface one typically finds such deformations to be of the order of 10^{-6} m which is comparable to the size of the particle. Hence such particles undergo substantial deformation at the interface, an aspect that has not been taken into account in the simulations of Groot and Stoyanov.

It is the purpose of this paper to address these issues by first determining the (equilibrium) equation of state (EOS) for PNIPAM microgel particles adsorbed onto an air-water interface using a Langmuir balance(LB). Second, we follow the time-dependent evolution of surface pressure in a separate experiment as PNIPAM particles adsorb from an aqueous bulk solution to the interface of newly formed air bubble using pendant drop (c.q. 'bubble') tensiometry. From these two measurements it is possible to obtain the kinetics of adsorption $\Gamma(t)$, revealing important aspects of the mechanisms controlling the adsorption kinetics.

2 Materials

The PNIPAM particles are synthesized by a batch suspension polymerization using a recipe that has been described in literature[17,18]. We used N-isopropyl acrylamide (NIPAM) as monomer with N, N-methylenebisacrylamide as the cross linker (2 mol$\%$) and potassium persulfate as the initiator for the polymerization reaction. We expect the particles to carry a small amount of charge due to the potassium persulfate used in the initiation step. The particles are purified by repeatedly centrifuging at 18000 g and replacing the supernatant with fresh Milli-Q water. The process was repeated at least 5 times. The particles are then freeze dried and stored. The suspension is prepared by weighing a calculated amount of the freeze dried particles and simply adding them to Milli-Q water to get the desired concentration and stirring for at least 24 hours before use. We prepare a stock solution of 0.5 g/l concentration. Suspensions of lower concentration are prepared by diluting this stock solution.

3 Methods

3.1 Particle Characterisation

The size of the microgels is measured by Dynamic Light Scattering on a Malvern Zeta Sizer. The hydrodynamic diameter of the particles at 20 °C is 589 $\pm$ 5 nm which, using the Stokes-Einstein relation, corresponds to a diffusion coefficient of 7.29×10^{-13} m^2/s. Calibrated Static Light Scattering is used to find the molar mass and the radius of gyration of these particles by fitting the form factor assuming the particle to be spherical. We use $dn/dC = 0.167$ ml/g as reported in literature[19]. The molar mass is 1.82×10^6 kg/mol and the radius of gyration (R_g) at 20 °C is 200 $\pm$ 19 nm. A small value of R_g / R_h indicates existence of long dangling chains on the periphery of a stiffer cross-linked core[20].

3.2 LB pressure-area isotherms

The equation of state (Pressure v/s Adsorbed mass relationship) is determined using a Langmuir trough. All the experiments are carried out at room temperature. Firstly we carefully clean the air water interface until a point where the pressure area compression cycle shows a perfectly horizontal line and the pressure at maximum compression is < 0.1 mN/m. We then spread a known amount of particles on a clean air-water interface and systematically reduce the area of the interface. The resultant change in pressure is recorded by a pressure sensor using a Wilhelmy plate. We perform 3 different sets of experiments: Two of these sets are performed on a NIMA Langmuir trough with a Mini PS4 pressure sensor using a paper Wilhelmy plate. The maximum and minimum possible areas available on the NIMA trough are 500 cm^2 and 40 cm^2 respectively. In the first set we study the particles at high initial loading. We spread 100 μl of a suspension of 0.5 g/l concentration. We carefully place the drops of the suspension on the interface using a 10 μl syringe with a sharp tip by holding the needle very close and parallel to the interface. We try to evenly deposit the drops over the initial spreading area and wait for at least 30 minutes for the system to stabilize before we begin our measurements. For the second set of experiments we use the same NIMA trough but this time we study the system at lower initial loading. We spread 40 μl of the 0.5 g/l concentration suspension. We carry out one more set of experiments on a Kibron μ-trough. The maximum and minimum possible areas in the Kibron μ-trough are 51.50 cm^2 and 3.25 cm^2, respectively. We spread 100 μl of 0.035 g/l particle solution on an initially clean air-water interface. These loading conditions are similar to the loading conditions for NIMA for high loading. The compression rate was kept low (10 cm^2/min for NIMA trough and 5 cm^2/min for Kibron μ-trough). The reproducibility of the experiments is checked by repeating the experiment under the same conditions. We also check for hysteresis between the compression and the expansion cycles. We find the hysteresis in the values of pressure to be < 2 mN/m. Compression-expansion cycles are repeated and no evidence for particle detachment is found in any experiment.

3.3 Interfacial tension measurements

We use a Dataphysics OCA apparatus to measure the surface tension of microgel particle laden interfaces. We create an air bubble in the suspensions of varying concentrations using an inverted needle. The interfacial tension (γ) is calculated with a resolution $\pm$ 0.01 mN/m by image analysis from the shape of the bubble using the well-known Laplace equation. We convert

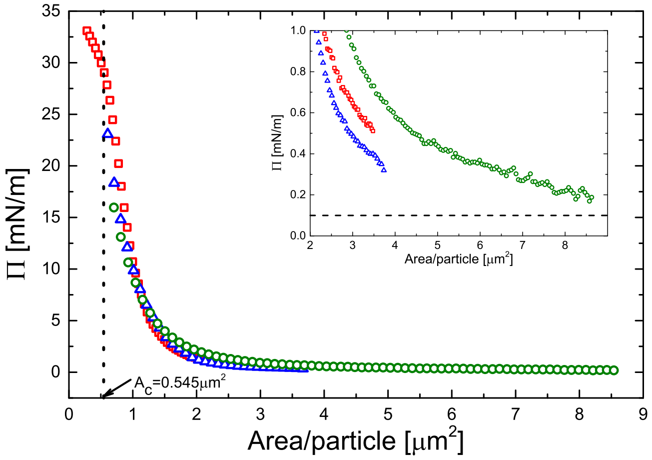

Fig. 1 Pressure area isotherm for PNIPAM particles at air-water interface. The open symbols denote experimental data points corresponding to three different sets of experiments namely: (□) NIMA trough with high initial particle loading, (○) NIMA trough with low initial particle loading and (△) Kibron μ-trough with high initial particle loading. Inset shows expanded view of the pressure area curve at low loadings. The dashed line in the inset denotes the detection limit of the pressure sensor.

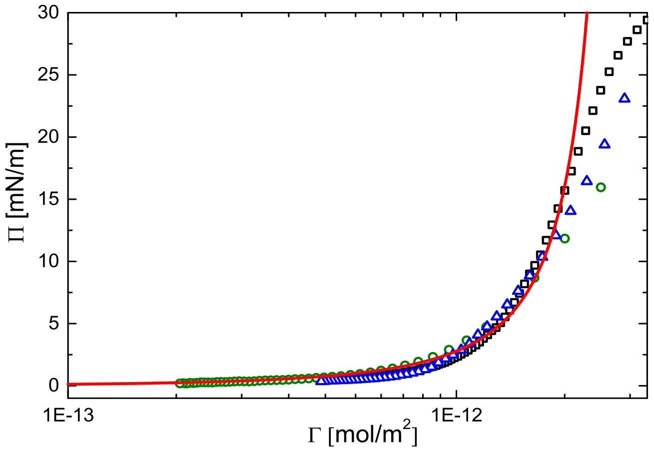

Fig. 2 Surface pressure(Π) v/s amount of PNIPAM particles adsorbed (Γ) on an air - water interface. The open symbols denote experimental data points corresponding to three different sets of experiments namely: (□) NIMA trough with high initial particle loading, (○) NIMA trough with low initial particle loading and (△) Kibron μ-trough with high initial particle loading. The solid red line denotes the predictions made using the Groot and Stoyanov model.

the values of interfacial tension into surface pressure by using the correlation $\Pi(t) = \gamma_0 - \gamma(t)$. Where $\gamma_0 = 72$ mN/m is the value of bare air-water interfacial tension. For the interfacial tension measurements to be accurate, we make sure that the bubble is big enough so that it is substantially deformed by the buoyancy forces. The Bond number is defined as $Bo = \Delta\rho g R^2/\gamma$, where, $\Delta\rho$ is the density difference between the fluids, R is the radius of the drop and γ is the interfacial tension. It is a measure of the interplay between the gravity/buoyancy and surface forces. For accurate measurements, it is advised that Bo should always lie between 0.1 and 1[21]; we check this to be the case in all our measurements. Like the surface pressure experiments, all tensiometry measurements are carried out at room temperature.

4 Results and Discussion

The pressure-area isotherms are obtained from compression of spread monolayers on a Langmuir trough for 3 different set of experiments. The area coordinates in these isotherms are scaled by the number of particles adsorbed on the interface. All the curves collapse on to a single plot as shown in Figure 1. At increasing compression, the pressure initially varies a little, but below 2 μm^2/particle, there is a steep increase in the pressure. The slope of the curve first increases, but reaches a maximum at $\sim$ 27 mN/m where there is an inflection point followed by a somewhat weaker slope. The value of area per particle (A_c) that corresponds to this inflection point turns out to be 0.545 μm^2 as shown by the dotted line in Figure 1. Assuming the particles are closely packed, this corresponds to an inter-particle distance of $\sim$ 835 nm, which is much larger than the hydrodynamic diameter of the particles measured in the bulk solution (590 nm) suggesting that the particles are indeed substantially deformed. As the inset of Figure 1 shows, finite surface pressures of order 0.5 mN/m (i.e. well above our detection limit of 0.1 mN/m) can in fact be measured already at areas per particle of around 4 μm^2. The inset also shows that the absolute values of Π are reproducible to within 0.3 mN/m between different experiments on the two different Langmuir troughs.

In Figure 2 we present the same data as in Figure 1, but converted into a Pressure v/s adsorbed amount curve using $\Gamma = 1/(\mathrm{A} \times \mathrm{N_{Av}})$ where A is the area/particle from Figure 1 and $\mathrm{N_{Av}}$ is the Avogadro number. This curve represents the 2D Equation of State (EOS) of the present system. At relatively low densities ($< 5 \times 10^{-13}\mathrm{mol/m^2}$) the pressure is extremely low (≈ 1mN/m) but quite well detectable. It follows that even at low densities where the inter-particle distance is much larger than the particle size in solution, the particles still somehow interact. As the particles hardly have any electrophoretic mobility[22,23], electrostatic repulsion is unlikely to be the cause. The only other option is particle-particle contact. Hence the particles must be strongly deformed upon their adsorption onto the interface, which qualitatively agrees with the findings by

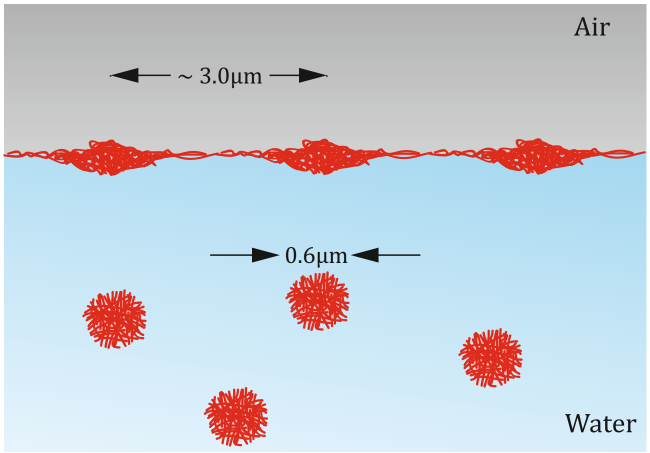

Fig. 3 Schematic representation of the deformation of microgel particles upon adsorption to the interface at very low loading conditions.

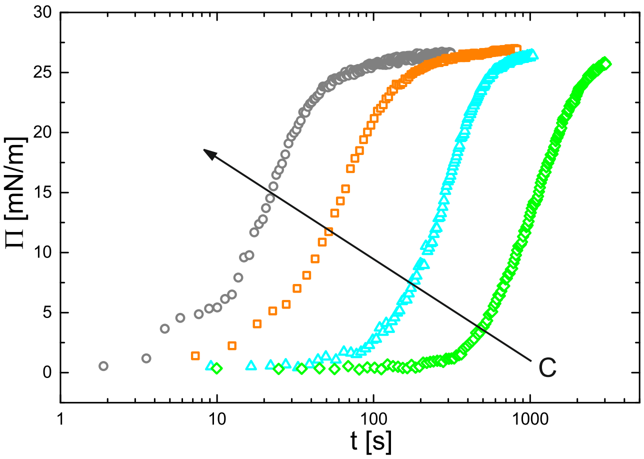

Fig. 4 Evolution of Surface pressure (Π) as a function of time. The open symbols are experimental data points. Different symbols and colors denote various bulk concentration of particles: (◇)0.10 g/l, (△)0.20 g/l, (□)0.50 g/l, (○)1.00 g/l. Arrow denotes the direction of increasing concentration

other authors[2,3,7,8,15,24]. We can make a rough estimate the extent of deformation using the ansatz $\Delta\mathrm{r} \approx \Delta\gamma/\varepsilon$. Using typical values of $\varepsilon \approx 50$ kPa from the literature[25,26] along with $\Delta\gamma = 70$ mN/m, we find $\Delta\mathrm{r} = 1.7\mu$m which is consistent with the distances of ~ 3 μm between close-packed and fully deformed particles. We base our analysis on the assumption that the particles that we spread on the interface do not desorb. But even if we accounted for desorption of particles, it would only mean that the finite pressures detected would in fact correspond to even lower surface concentrations. Figure 3 shows a schematic explanation of the mechanism of deformation of the particles at the interface. It should be noted that in case of LB experiments, the particles are spread on the interface and we do not have any particles in the bulk. In case of the interfacial tension measurements, the particles diffuse from the bulk to the interface.

Particles adsorbing to a fluid-fluid interface interact with each other and give rise to the surface pressure (Π), which is the 2D analogue of pressure in 3D systems. By extending this analogy further, it is also possible to relate this surface pressure to other state parameters like the number density and temperature via an equation of state. For colloidal particles adsorbing on a fluid-fluid interface, the simplest approximation could be that of 2D hard disks. The equation of state (EOS) for a one component system is given in terms of density dependence of the compressibility factor Z. The literature is replete with multiple approaches towards providing an expression for an EOS for 2D hard disk fluid. Mulero et.al.[27,28] provide a succinct review and comparison of all these equations of state.

We find that at very low densities the surface pressure measured is at least 5-6 orders of magnitude higher than predictions of surface pressures assuming an ideal gas of non-interacting particles at these densities. Groot and Stoyanov[13] do not explicitly consider the deformation of these particles due to surface tension. They simply postulate that the pressure depends predominantly on the micro-structure and composition of polymers within the colloidal particles, and introduce a new length scale $\mathrm{d_{eff}}$ which is meant to reflect the particle micro-structure, and which up scales the pressure to experimental values. However, realizing that the particles spread out to a large extent, we can also see the measured pressure as reflecting the internal elasticity of the particles. Since this is given by a 2D density of crosslinks, it is not surprising that we find a microscopic length.

Groot and Stoyanov propose an expression for surface pressure(Π) that takes into account the size of these smaller correlated domains within the particle given by:

$$\Pi = \frac{4k_\mathrm{B}\mathrm{T}}{\pi \mathrm{d_{eff}}^2}\left(\frac{b\eta \mathrm{Z}(\lambda\eta)}{\lambda} - b_2\eta^2\right) \tag{1}$$

where, $\mathrm{d_{eff}}$ is the size of the correlated domains within the particle. The compressibility factor (Z) can be expressed by using any of the equations of state available in literature. In our case, we use the modified Henderson equation[29] given by:

$$\mathrm{Z_{HM}} = \frac{1+\eta^2/8}{(1-\eta)^2} - \frac{0.043\eta^4}{(1-\eta)^3} \tag{2}$$

where η is the surface packing fraction which can in turn be expressed in terms of the number density of particles (ρ) and the bulk diameter of individual particle (d) as $\eta = (\pi/4)\rho \mathrm{d}^2$. For our experiments, η lies between 0 and 0.91. The corresponding values of $\mathrm{Z_{HM}}$ lie between 1 and 96.

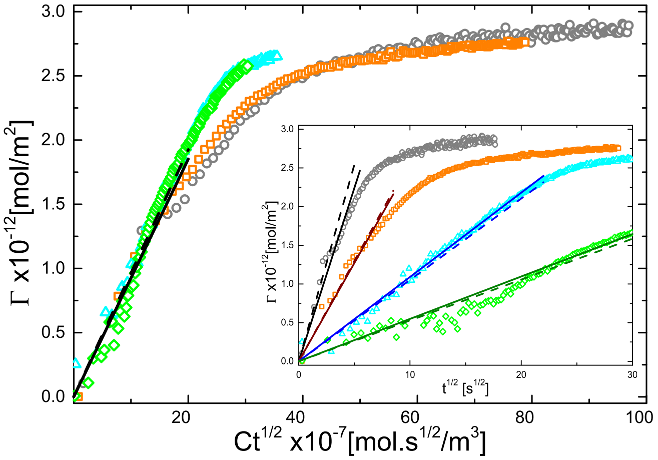

Fig. 5 Adsorbed amount(Γ)as a function of the product $Ct^{1/2}$. The inset shows the individual curves of Γ v/s $t^{1/2}$ for various bulk concentration of microgel particles: (◇)0.10 g/l, (△)0.20 g/l, (□)0.50 g/l, (○)1.00 g/l. Solid lines are straight line fits and dashed lines are drawn with slopes calculated using $D = D_{\mathrm{DLS}}$

Table 1 Values of diffusion co-efficient D (m^2/s) for various concentrations calculated from the experimental Γ v/s $t^{1/2}$ curves compared to ones measured using DLS.

Conc(g/l)	Conc(mol/m^3)	$D_{\mathrm{exp}}(m^2/s)$	$D_{\mathrm{DLS}}(m^2/s)$
0.10	5.495×10^{-8}	7.57×10^{-13}	7.26×10^{-13}
0.20	1.099×10^{-7}	7.73×10^{-13}	7.20×10^{-13}
0.50	2.747×10^{-7}	6.72×10^{-13}	7.01×10^{-13}
1.00	5.495×10^{-7}	6.48×10^{-13}	6.72×10^{-13}

We fit the scaling relation given by Groot and Stoyanov to our data in Figure 2(red curve). The fitting gives d_{eff} = 1.25 nm as the characteristic length scale. To provide a physical picture, this d_{eff} can be viewed as the average distance between crosslinks within the microgel particle. This is in agreement with previous studies[30,31] that report a mesh size in the range of 1 - 10 nm. The parameters b and λ used in the model denote repulsive interactions due to the elastic nature of disks. For our system, the values for b and λ can be taken as unity[13]. The parameter b_2 denotes short range attractive interactions. We checked the effect of short range attraction interaction by incorporating the parameter b_2 as a fit parameter, but the analysis yields extremely small values of b_2 $(\sim 1 \times 10^{-4})$. Hence we conclude that we have purely repulsive particles. The deviations of the actual data from the model at high loading are possibly because at high compressions, the surface no longer remains flat but undergoes out-of-plane deformations i.e., buckles. Also, these particles have a lot of loose, un-crosslinked polymer chain segments along the periphery of these particles. At high compressions, it is energetically favourable for these segments to leave the interface rather than inter-penetrate. Such partial desorption also may result in deviations from the predictions of hard disk like model.

Having established an equation of state to correlate the surface pressure and the adsorbed amount, we now proceed to study the adsorption dynamics of the particles. For this we monitor the evolution of the interfacial tension of a freshly prepared air bubble in a suspension of PNIPAM particles as a function of time. We convert the values of interfacial tension into surface pressure. The results are as shown in Figure 4. The values of surface pressure initially increase rapidly and then relax to a final equilibrium value. The dynamics can be clearly separated into two separate time scales: An initial rapid dynamics denoted by the increase in the surface pressure values, and a slow part as the system relaxes towards the final equilibrium state. This distinction between rapid kinetics at short times and much slower kinetics at longer times is characteristic for the adsorption behavior of many surface active materials[32,33].

At short time scales, the increase in Π is limited by the transport of the particles from the bulk to the interface. We expect the transport to be governed by the diffusion of particles. Since our particles are fairly large, the energy of adsorption for these particles is 3-4 orders of magnitude higher than k_BT. Hence it is safe to assume that the particles never leave the interface once they are adsorbed. Under these conditions, the Ward and Tordai model[34] gives:

$$\Gamma = 2C\sqrt{\frac{Dt}{\pi}} \tag{3}$$

where, Γ is the adsorbed molar mass, C is the bulk concentration and D is the diffusion co-efficient of the particles.

Using the experimental Π v/s Γ curves obtained in Figure 2, we convert the Π(t) data into Γ(t) data and then plot Γ v/s C $t^{1/2}$ as shown in Figure 5. We scale the time axis with concentration expecting the curves to collapse onto a single curve. What we observe is that the initial growth of Γ follows the $t^{1/2}$ dependence quite well. This is followed by a concentration dependent slowing down in the relaxation of Γ at long times as the system approaches saturation. The inset in Figure 5 shows the individual Γ v/s $t^{1/2}$ curves for different bulk concentration of particles. The solid lines are straight line fits to the initial part of the experimental data (open symbols). The initial slope of each curve yields a value for the diffusion coefficient D. For comparison, the dashed lines are drawn with slopes calculated using D obtained from Dynamic Light Scattering (DLS) $(D_{\mathrm{DLS}} = 7.29 \times 10^{-13} m^2/s)$. As can be seen, they do not deviate very much from the experimental curves. Alternatively,

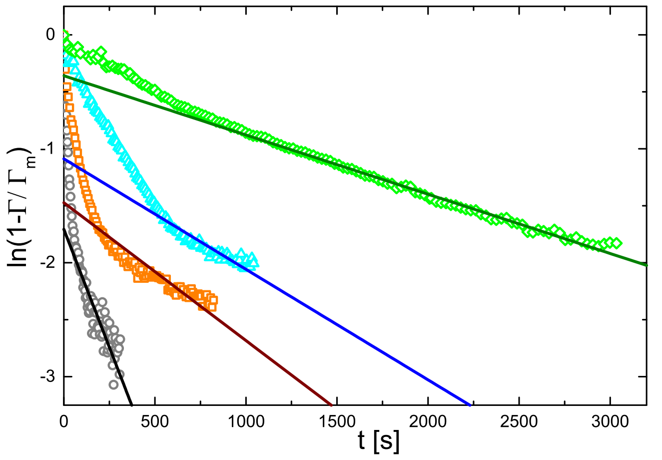

Fig. 6 ln(1 - Γ/Γ_m) as a function of time for various bulk concentration of microgel particles: (◇)0.10 g/l, (△)0.20 g/l, (□)0.50 g/l, (○)1.00 g/l. Solid lines are straight line fits.

we can determine D from best fits to the data. Table 1 gives the values of D as obtained by fitting straight lines (solid lines) to the experimental results for different bulk concentration and compares them to the value obtained from DLS. The values so obtained do not deviate by more than 10% from the ones measured by DLS.

As the system approaches saturation, the fall in Γ(t) must slow down as the surface gets crowded. The concentration of the adsorbate just below the surface then falls out of equilibrium with the adsorbed species and the kinetics becomes limited by an adsorption barrier. A first order kinetic process then leads to:

$$\frac{d\Gamma}{dt} \sim k\left(\Gamma_{\max} - \Gamma\right) \tag{4}$$

where, k is the rate constant that is related to the adsorption barrier. Ideally, k should be proportional to the local solute concentration below the interface. This leads to an exponential relaxation:

$$\Gamma = \Gamma_{\max}\left(1 - \mathrm{e}^{-kt}\right) \tag{5}$$

Figure 6 shows that such a barrier controlled regime does indeed exist at long times. The open symbols are the experimental values for $ln(1 - \Gamma/\Gamma_{\max})$. At long times, the curves fit a straight line as denoted by the solid lines. The slopes of the solid lines can be identified to the inverse of a kinetic relaxation time which is $1/k$.

As shown in Table 2, the rate constant depends on the bulk concentration of the microgel particles. But the dependence is not linear. This presumably indicates that the adsorption process itself is rather complex and depends on details of the configuration of the particles at the interface. A deeper analysis of these aspects is beyond the scope of the present work.

Table 2 Values of rate constant $k(1/\mathrm{s})$ for various concentrations calculated from the experimental curves in Fig 6.

Conc(g/l)	Conc(mol/m^3)	$k(1/\mathrm{s})$
0.10	5.495×10^{-8}	5.21×10^{-4}
0.20	1.099×10^{-7}	9.70×10^{-4}
0.50	2.747×10^{-7}	1.21×10^{-3}
1.00	5.495×10^{-7}	4.13×10^{-3}

5 Conclusions

PNIPAM microgels adsorb readily to an air-water interface owing to their polymeric nature. We have experimentally established a 2D equation of state for such soft microgel particles adsorbed onto an air water interface. The pressure area isotherms give a measurable pressure even at average interparticle distances much larger than their hydrodynamic diameter in the bulk. This confirms the fact that the particles deform substantially at the interface. Using a simple scaling argument we show that the deformation of particles is of the same order as the inter-particle distance at very low loadings resulting in a very small yet measurable pressure. This pressure at low loadings indirectly probes the internal elasticity of the particles, which is related to the internal cross link density. Experimental observations of an EOS match the scaling relation proposed by Groot and Stoyanov. The length scale $\mathrm{d_{eff}}$ = 1.25 nm that arises out of this scaling relation can be seen as an effective distance between the crosslinks. The deviations from the scaling relation at very high loadings may be attributed to buckling of the interfacial layer or to partial desorption of the peripheral polymeric chain segments due to compression.

Using the experimental EOS, we study the adsorption dynamics of these microgel particles on to air-water interface. We find that the adsorption process can be clearly separated into two regimes. At short times, the adsorption process is controlled by the diffusion of the particles from bulk to the interface. At long times, the interface gets filled with particles thereby creating a barrier for newer particles to adsorb onto the interface. This leads to an exponential relaxation of Γ.

Acknowledgements

We would like to thank Prof. Vinod Subramaniam for letting us use the Kibron μ-trough and Mr. Aditya Iyer with his help in the experiments on the Kibron μ-trough. We also thank Dr. Arun Banpurkar for his ideas and discussions. This work has been supported by the Foundation for Fundamental research on Matter (FOM), which is financially supported by the Netherlands Organization for Scientific Research (NWO).

References

1 B. Brugger and W. Richtering, *Langmuir*, 2008, **24**, 7769–7777.

2 B. Brugger, B. A. Rosen and W. Richtering, *Langmuir*, 2008, **24**, 12202–12208.

3 M. Destribats, V. Lapeyre, M. Wolfs, E. Sellier, F. Leal-Calderon, V. Ravaine and V. Schmitt, *Soft Matter*, 2011, **7**, 7689–7698.

4 B. P. Binks, *Current Opinion in Colloid & Interface Science*, 2002, **7**, 21–41.

5 L. A. Lyon and A. Fernandez-Nieves, *Annual Review of Physical Chemistry*, 2012, **63**, 25–43.

6 B. Brugger, J. Vermant and W. Richtering, *Physical Chemistry Chemical Physics*, 2010, **12**, 14573–14578.

7 M. Destribats, V. Lapeyre, E. Sellier, F. Leal-Calderon, V. Ravaine and V. Schmitt, *Langmuir*, 2012, **28**, 3744–3755.

8 K. Geisel, L. Isa and W. Richtering, *Langmuir*, 2012, **28**, 15770–15776.

9 Z. Li, K. Geisel, W. Richtering and T. Ngai, *Soft Matter*, 2013, **9**, 9939–9946.

10 T. Ngai, S. H. Behrens and H. Auweter, *Chemical Communications*, 2005, 331–333.

11 Y. Cohin, M. Fisson, K. Jourde, G. Fuller, N. Sanson, L. Talini and C. Monteux, *Rheologica Acta*, 2013, **52**, 445–454.

12 S. L. Kettlewell, A. Schmid, S. Fujii, D. Dupin and S. P. Armes, *Langmuir*, 2007, **23**, 11381–11386.

13 R. D. Groot and S. D. Stoyanov, *Soft Matter*, 2010, **6**, 1682–1692.

14 S. Höfl, L. Zitzler, T. Hellweg, S. Herminghaus and F. Mugele, *Polymer*, 2007, **48**, 245 – 254.

15 M. Destribats, M. Eyharts, V. Lapeyre, E. Sellier, I. Varga, V. Ravaine and V. Schmitt, *Langmuir*, 2014.

16 M. Horecha, V. Senkovskyy, A. Synytska, M. Stamm, A. I. Chervanyov and A. Kiriy, *Soft Matter*, 2010, **6**, 5980–5992.

17 R. Acciaro, T. Gilanyi and I. Varga, *Langmuir*, 2011, **27**, 7917–7925.

18 X. Wu, R. H. Pelton, A. E. Hamielec, D. R. Woods and W. McPhee, *Colloid and Polymer Science*, 1994, **272**, 467–477.

19 S. Zhou, S. Fan, S. C. F. Au-yeung and C. Wu, *Polymer*, 1995, **36**, 1341–1346.

20 I. Varga, T. Gilnyi, R. Mszros, G. Filipcsei and M. Zrnyi, *The Journal of Physical Chemistry B*, 2001, **105**, 9071–9076.

21 R. de Ruiter, R. W. Tjerkstra, M. H. G. Duits and F. Mugele, *Langmuir*, 2011, **27**, 8738–8747.

22 M. Garcia-Salinas, M. Romero-Cano and F. de las Nieves, *Journal of Colloid and Interface Science*, 2001, **241**, 280 – 285.

23 O. S. Deshmukh, A. Maestro, M. H. G. Duits, D. van den Ende, M. Cohen Stuart and F. Mugele, Manuscript in preparation.

24 W. Richtering, *Langmuir*, 2012, **28**, 17218–17229.

25 A. Burmistrova, M. Richter, M. Eisele, C. zm and R. von Klitzing, *Polymers*, 2011, **3**, 1575–1590.

26 E. H. Purnomo, D. van den Ende, S. A. Vanapalli and F. Mugele, *Phys. Rev. Lett.*, 2008, **101**, 238301.

27 *Theory and Simulation of Hard-Sphere Fluids and Related Systems*, ed. A. Mulero, Springer, Berlin, 2008.

28 A. Mulero, I. Cachadia and J. R. Solana, *Molecular Physics*, 2009, **107**, 1457–1465.

29 D. Henderson, *Molecular Physics*, 1977, **34**, 301–315.

30 C. Fänger, H. Wack and M. Ulbricht, *Macromolecular Bioscience*, 2006, **6**, 393–402.

31 S. Sun and P. Wu, *J. Mater. Chem.*, 2011, **21**, 4095–4097.

32 C. H. Chang and E. I. Franses, *Colloids and Surfaces A: Physicochemical and Engineering Aspects*, 1995, **100**, 1 – 45.

33 H. Ritacco, D. Langevin, H. Diamant and D. Andelman, *Langmuir*, 2011, **27**, 1009–1014.

34 A. F. H. Ward and L. Tordai, *The Journal of Chemical Physics*, 1946, **14**, 453–461.

Table of contents entry

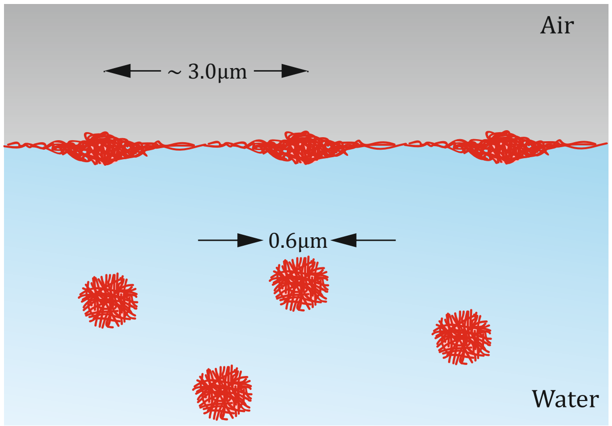

PNIPAM microgel particles deform substantially upon adsorbing onto an air-water interface. The adsorption is initially controlled by the diffusion of particles to the interface followed by a slow exponential relaxation at long times.